**molecular
systems
biology**

Coordination of frontline defense mechanisms under severe oxidative stress

Amardeep Kaur[1], Phu T Van[1], Courtney R Busch[2], Courtney K Robinson[2], Min Pan[1], Wyming Lee Pang[1], David J Reiss[1], Jocelyne DiRuggiero[2] and Nitin S Baliga[1,*]

[1] Institute for Systems Biology, Seattle, WA, USA and [2] Department of Biology, Johns Hopkins University, Baltimore, MD, USA
* Corresponding author. Baliga Lab, Institute for Systems Biology, 1441 North 34th Street, Seattle, WA 98103, USA.
Tel.: + 1 20 67 32 1266; Fax: + 1 20 67 32 1299; E-mail: nbaliga@systemsbiology.org

Complexity of cellular response to oxidative stress (OS) stems from its wide-ranging damage to nucleic acids, proteins, carbohydrates, and lipids. We have constructed a systems model of OS response (OSR) for *Halobacterium salinarum NRC*-1 in an attempt to understand the architecture of its regulatory network that coordinates this complex response. This has revealed a multi-tiered OS-management program to transcriptionally coordinate three peroxidase/catalase enzymes, two superoxide dismutases, production of rhodopsins, carotenoids and gas vesicles, metal trafficking, and various other aspects of metabolism. Through experimental validation of interactions within the OSR regulatory network, we show that despite their inability to directly sense reactive oxygen species, general transcription factors have an important function in coordinating this response. Remarkably, a significant fraction of this OSR was accurately recapitulated by a model that was earlier constructed from cellular responses to diverse environmental perturbations—this constitutes the general stress response component. Notwithstanding this observation, comparison of the two models has identified the coordination of frontline defense and repair systems by regulatory mechanisms that are triggered uniquely by severe OS and not by other environmental stressors, including sub-inhibitory levels of redox-active metals, extreme changes in oxygen tension, and a sub-lethal dose of γ rays.
Molecular Systems Biology **6**: 393; published online 27 July 2010; doi:10.1038/msb.2010.50
Subject Categories: metabolic and regulatory networks; microbiology and pathogens
Keywords: gene regulatory network; microbiology; oxidative stress

Introduction

Reactive oxygen species (ROS), such as hydrogen peroxide (H_2O_2), superoxide (O_2^-), and hydroxyl (OH^-) radicals are normal by-products of aerobic metabolism. Evolutionarily conserved mechanisms including detoxification enzymes (peroxidase/catalase and superoxide dismutase (SOD)) and free radical scavengers manage this endogenous production of ROS. Oxidative stress (OS) is a condition reached when certain environmental stresses or genetic defects cause the production of ROS to exceed the management capacity. The damage to diverse cellular components including DNA, proteins, lipids, and carbohydrates resulting from OS (Imlay, 2003; Apel and Hirt, 2004; Perrone *et al*, 2008) is recognized as an important player in many diseases and in the aging process (Finkel, 2005).

A great deal of information exists on specific detoxification enzymes, ion scavengers, and their associated regulators. For instance, in *Eshcherichia coli*, it is known that the *oxyR* regulon is induced by higher levels of H_2O_2, whereas the *soxRS* regulon is activated by exposure to redox-cycling agents (Zheng and Storz, 2000; Green and Paget, 2004; Imlay, 2008). Activation of many of these regulators by metals, radiation, and starvation conditions shows how diverse environmental factors (EFs) can directly or indirectly increase production of ROS. Not surprisingly, the regulation of OS response (OSR) is tied to circuits that manage diverse processes including metal trafficking, nutrient transport, and general aspects of metabolism. The function of metal trafficking is especially important given the function of transition metals, iron in particular, in the production of highly reactive OH^- through the Fenton reaction. It is clear from all of these earlier studies that a systems approach will be necessary to fully appreciate the highly interconnected nature of the regulatory networks that manage OSR (Temple *et al*, 2005).

Given that many archaea thrive in extreme environments associated with elevated production of ROS, it is intriguing to consider these organisms as models for characterizing global regulatory networks that efficiently manage extreme OS during normal metabolism (Joshi and Dennis, 1993; Kawakami *et al*, 2004; Limauro *et al*, 2008). Furthermore, although archaeal transcriptional regulation is mediated by regulators of bacterial ancestry, many of the known bacterial OSR regulators are absent in this domain of life (Coulson *et al*, 2007). Here, we have applied a systems approach to characterize the OSR of an archaeal model organism, *Halobacterium salinarum NRC-1*. This haloarchaeon grows aerobically at 4.3 M salt concentration in which it routinely faces cycles of desiccation and rehydration, and increased ultraviolet radiation—both of which can increase the production of ROS (Farr and Kogoma, 1991; Oliver *et al*, 2001). We have reconstructed the physiological adjustments associated with management of excessive OS through the analysis of global dynamic transcriptional changes elicited by constant exposure to growth sub-inhibitory and sub-lethal levels of H_2O_2 and paraquat (PQ—a redox-cycling drug that produces O_2^-; Hassan and Fridovich, 1979) as well as during subsequent recovery from these stresses. We have integrated all of these data into a unified model for OSR to these ROS to discover conditional functional links between protective mechanisms and normal aspects of metabolism. Subsequent phenotypic analysis of gene deletion strains has verified the conditional detoxification functions of three putative peroxidase/catalase enzymes, two SODs, and the protective function of rhodopsins under increased levels of H_2O_2 and PQ. Similarly, we have also validated ROS scavenging by carotenoids and flotation by gas vesicles as secondary mechanisms that may minimize OS. Although it has been known that OS is a component of diverse environmental stress conditions, we quantitatively show for the first time that much of the transcriptional responses induced by the two treatments could indeed have been predicted using a model constructed from the analysis of transcriptional responses to changes in other EFs (UV and γ-radiation, light, oxygen, and six metals). However, using specific examples, we also reveal the specific components of the OSR that are triggered only under severe OS. Notably, this model of OSR gives a unified perspective of the interconnections among all of these generalized and OS-specific regulatory mechanisms.

Results and discussion

We present the results and discussion in six sections (A–F) starting with (A) characterization of growth and survival characteristics of *H. salinarum NRC-1* under increasing doses of H_2O_2 and PQ, (B) analysis of global dynamic transcriptional responses to selected sub-inhibitory and sub-lethal doses of the two stressors, (C) inference of a globally integrated model of conditionally co-regulated genes and their sub-circuits, (D) experimental validation of important hypotheses regarding primary and secondary defense mechanisms and their functional relationships, (E) statistical evaluation of generalized and specific aspects of OS management, and (F) summary of the integrated program for OS management.

Distinct differences in phenotypic responses to H_2O_2 and PQ

We first characterized survival and growth characteristics of *H. salinarum NRC-1* with increasing doses of H_2O_2 and O_2^-. Although peroxide stress was generated by directly adding H_2O_2 to a desired concentration (titration doses for survival studies: 0–40 mM; growth studies: 0–7 mM), O_2^- radicals were generated indirectly during metabolism of exogenously added PQ (titration doses for survival studies: 0–10 mM; growth studies: 0–0.5 mM) (Hassan and Fridovich, 1979) (Figure 1). Interestingly, the cells withstood exogenously added H_2O_2 stress up to a concentration of ∼30 mM beyond which their survival dropped precipitously. This sharp transition was also observed at the level of growth wherein the cells grew normally in up to 5–6 mM H_2O_2 and a smallest increase thereafter resulted in complete growth inhibition. This indicates that in the absence of earlier conditioning to low doses of OS (Cabiscol *et al*, 2000; Brioukhanov *et al*, 2006; Limauro *et al*, 2006), there exists a threshold to the cellular capacity to detoxify H_2O_2 and that even traces of peroxide beyond this threshold can result in devastating oxidative damage to cellular components. This phenotypic behavior under H_2O_2 stress is in stark contrast to the gradual loss in survival and growth observed under increasing O_2^- stress. The growth and survival assays aided in the selection of appropriate concentrations of H_2O_2 and PQ for subsequent transcriptomic analysis. The enormous amount of the two stress agents required to achieve sub-lethal effects is a testament to the remarkable capacity of this organism to efficiently eliminate and keep intracellular concentration of ROS within physiologically acceptable limits.

Global transcriptional analysis reveals shared and specific responses to peroxide and O_2^-

We sought to model OSR at a systems scale by characterizing OS-management mechanisms and unraveling the gene regulatory programs that coordinate their operation with other aspects of metabolism. We approached this problem by charting dynamic global transcriptional changes for up to 4 h during and after exposure to sub-lethal concentrations of each PQ (4 mM) and H_2O_2 (25 mM) that resulted in 20–30% loss of survival (Figure 2; Supplementary Figures S1 and S2; Supplementary Tables S1–S3). Further, we also characterized transcriptional responses during nearly 6 h of acclimation to a growth sub-inhibitory dose of PQ (0.25 mM) (this was not possible for peroxide stress owing to the sharp transition in growth with small concentration increases of H_2O_2) (Supplementary Figure S3; Supplementary Table S4). Together with control experiments and replicates, this represented nearly 300 high-density microarray experiments. We summarize discoveries from integrated analyses of data from these experiments (Materials and methods) (Supplementary Figure S1).

Exposure to both ROS resulted in differential regulation of a larger proportion of genes over time involving up to 50% of all genes at steady state. In contrast, transcriptional changes became somewhat subdued over time during recovery from both OS conditions (Supplementary Figure S1). Nearly half of
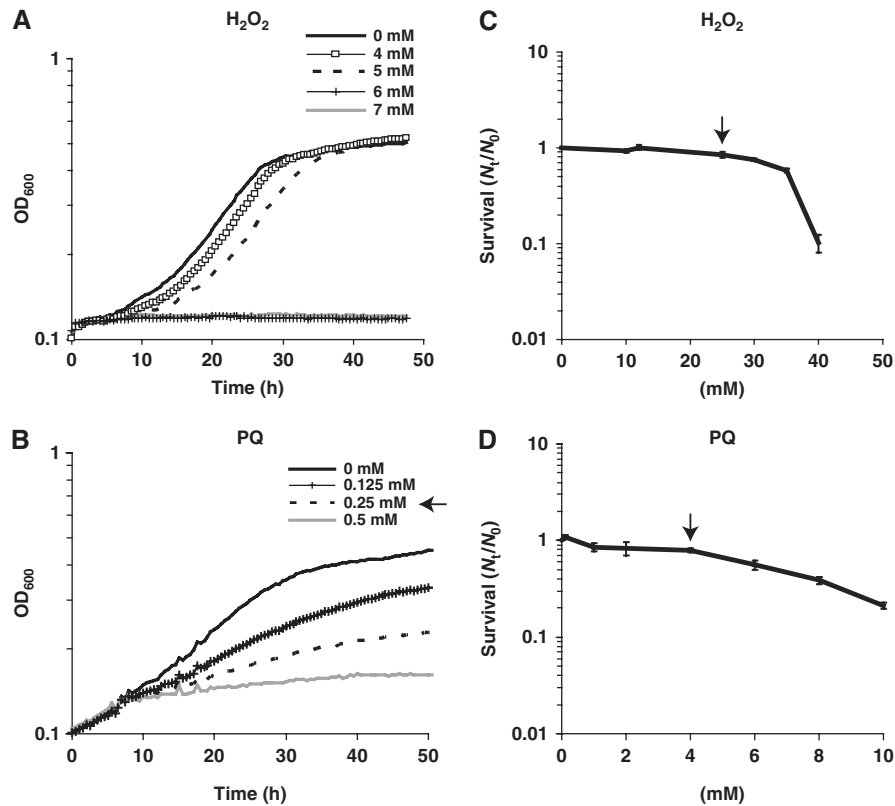
Figure 1 Growth and survival of *H. salinarum NRC-1* with H_2O_2 and PQ. Effect of increasing concentrations of H_2O_2 and PQ on growth (**A**, **B**) and survival (**C**, **D**) of *H. salinarum NRC-1* in complete media (CM). Growth was measured by determining increase in cell density (OD_{600}) at 30 min intervals using a Bioscreen instrument. Survival was calculated as ratio of number of viable cells (*N*) after 2 h treatment with varying doses of H_2O_2 or PQ to number of viable cells (N_o) in control. Black arrows represent dosage at which microarray analyses were performed. Data shown is representative of the experiments, which were repeated three times.

all differentially regulated genes (563 genes) were shared by the two stress responses—perhaps reflecting a generalized OS component (Supplementary Table S1). Notably, differential regulation of an equivalent fraction of genes (H_2O_2: 366 genes; PQ: 536 genes) was unique to each response. Some unique aspects of responses to the two ROS and between responses to sub-lethal and sub-inhibitory doses of PQ are noted in the Supplementary information (Figure 2; Supplementary Figures S2 and S3). By simultaneously analyzing putative functional assignments (Bonneau *et al*, 2004) and transcriptional changes, we have reconstructed physiological consequences of long-term exposures to and recovery from excessive H_2O_2 and O_2^- stress (Figure 2; Supplementary Figures S1–S3; Supplementary Tables S2–S4). We provide a summary of this analysis with emphasis on OS-related functions; observations pertaining to adjustments in general aspects of physiology including ribosome biogenesis, oxidative phosphorylation, and carbohydrate and nucleotide metabolism during the OSR are summarized in the Supplementary information.

ROS scavenging and detoxification
Many of the primary OS-management systems including detoxification by SODs, peroxidase/catalase, and peroxiredoxins, and radical scavenging by antioxidants, and reduction of radicals by redoxins (Storz and Imlay, 1999; Grant, 2001; Zheng *et al*, 2001; Toledano *et al*, 2007; Imlay, 2008) were

upregulated by both treatments (Figure 2O, P and S; Supplementary Table S2). Notably, in addition to upregulation of the classic peroxidase/catalase [*VNG6294G (perA)*— PF00141], we observed transcriptional induction of at least two additional enzymes of related function—*VNG0798H*, a putative dye-decolorizing peroxidase (PF04261, COG2837) (Sugano *et al*, 2007; Scheibner *et al*, 2008) and *VNG0018H*, whose predicted structure matches that of catalase [PDB: 1cf9A2; (Mate *et al*, 1999)]. *VNG1190G (sod1)* and peroxiredoxins [*VNG1197G (bcp)*, *VNG2311H*] were upregulated to a higher degree with PQ than with H_2O_2, suggesting that different regulatory circuits are responsible for managing ROS generated by the two treatments (Brioukhanov *et al*, 2006; Limauro *et al*, 2006, 2008). Upregulation of a number of other processes was also consistent with their functions in relation to OS including carotenoid synthesis [*VNG1458G (crtB1)*, *VNG1755G (crtI2)*] and glycerol metabolism [*VNG6277G (ugpB)*, *VNG6279G (ugpA)*, *VNG1967G (glpK)*, *VNG6270G (gldA)*] (Pahlman *et al*, 2001) (Figure 2A, B, and N).

Repair of oxidative damage
Although DNA repair mechanisms were in general regulated in a similar manner by both agents (Figure 2T; Supplementary Table S2), PQ treatment uniquely upregulated certain repair and recombination genes including *VNG2473G (radA1)*, ssDNA binding (*VNG1255C* and *VNG 2160C*), and DNA
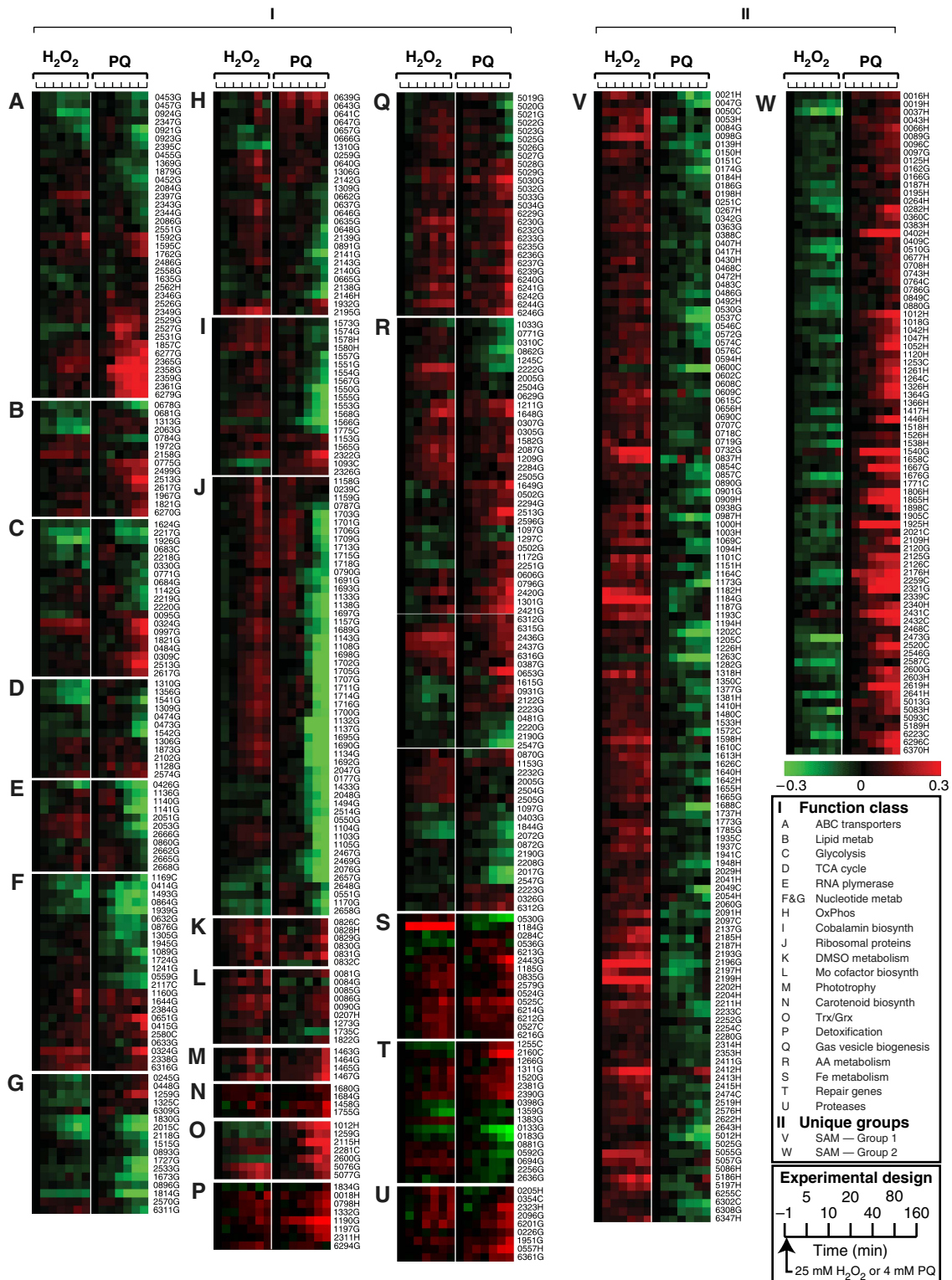
Figure 2 Temporal transcriptome changes in *H. salinarum NRC-1* treated with sub-lethal doses of H_2O_2 (25 mM) or PQ (4 mM). Relative changes in transcription of all genes were measured immediately before and up to 160 min after adding 25 mM H_2O_2 or 4 mM PQ. The mRNA $\log_{10}$ ratios were normalized to the first condition (control) and data were filtered ($\log_{10}$ ratio > 0.05, $\lambda=15$ in at least one condition; see Materials and methods for details). I. Differentially regulated genes are grouped into different functional groups (**A–U**) (see Supplementary Table S2 for details). II. Transcriptional profiles that distinguished OSRs to H_2O_2 and PQ (Groups **V** and **W**) were identified using the significance analysis of microarrays (SAM) algorithm (Tusher *et al*, 2001).

helicase [*VNG1406G* (*rhl*)]. Although it is clear from upregula-tion of proteases [*VNG0205H*, *VNG0354C*, VNG2096G (*cctB*), VNG0226G (*htrA*), *VNG1951G* (*sub*), *VNG2323H*, VNG6201G (*hsp5*), VNG6361G (*npa*)] that protein degradation was upregulated by both treatments (Figure 2U), it was striking that unlike the upregulation of ribosomal genes for replacing damaged proteins (Thorpe *et al*, 2004) under H_2O_2 stress, these genes were downregulated with PQ—even after the stress was taken away. We speculate that the sub-lethal dose of PQ (4 mM) was more damaging to proteins relative to H_2O_2 (25 mM), despite their comparable phenotypic effects (20–30% loss in survival). This is not surprising as PQ primarily generates O_2^- ions, which are known to be particularly deleterious to proteins as they increase the production of highly reactive OH^- radicals through the Fenton reaction by releasing free Fe^{2+} from solvent-exposed 4Fe-4S cluster of labile dehydratases (Imlay, 2003). As expected, lowering the dose of PQ to sub-inhibitory levels induced transcription of both proteases *and* ribosome biogenesis (Supplementary Figure S3).

Regulation of Fe–S metabolism

Most transcriptional changes induced by both treatments were over-represented for Fe-dependent and Fe–S-containing enzymes (Supplementary Figure S4; Supplementary Tables S5 and S6). For instance, a simple analysis of Fe–S cluster-associated motif-containing proteins shows that six of eight ($P=0.1$) putative electron transfer system proteins ($CX_2CX_2CX_3C$) and seven of nine ($P=0.08$) putative enzymes requiring S-adenosylmethionine (SAM) (CX_3CX_2C) were dif-ferentially expressed under OS (Supplementary Tables S5 and S6). This is not surprising as Fe–S clusters are used as cofactors by many redox proteins, radical SAM enzymes, and RNA polymerase (Boyd *et al*, 2009), and are important for electron transfer reactions and gene regulation as they sense changes in Fe, O_2, and O_2^- (Fontecave, 2006; Outten, 2007) (Figures 2, 3; Supplementary Tables S2 and S3). It has been proposed that conversion of Fe^{2+} to Fe^{3+} could trigger three types of responses: a Fe-deficiency such as response to bring in more Fe into the cell; an effort to repair or re-synthesize proteins with damaged Fe–S clusters and S-containing amino acids; and a protective response to sequester Fe in a non-reactive form (Varghese *et al*, 2007; Imlay, 2008). Consistent with this, cellular effort to scavenge and sequester Fe, and simulta-neously repair both damaged Fe–S clusters and S-containing amino acids was reflected in the upregulation of genes encoding Fe-scavengers: [putative siderophore biosynthesis [*VNG6213G* (*iucB*), *VNG6212G* (*iucA*), *VNG6214G* (*hxyA*), *VNG6216G* (*iucC*)] (Imlay, 2006)]; iron sequestration [ferritin [*VNG2443G* (*dpsA*)] (Andrews *et al*, 2003; Reindel *et al*, 2006; Shukla, 2006)]; S uptake [*VNG1592G* (*cysT2*)]; assembly of Fe–S clusters [*VNG0524G* (*yurY*), *VNG0525C*, *VNG0527C*] (Takahashi and Tokumoto, 2002; Loiseau *et al*, 2003); biosynthesis of cysteine and methionine [*VNG0796G* (*cgs*), *VNG2420G* (*metA*), *VNG2421G* (*hal*), and *VNG1301G* (*cysK*)]; and repair of oxidized cysteines and methionines [*VNG1180G* (*msrA*)] (Stadtman *et al*, 2003; Stadtman, 2006; Metayer *et al*, 2008) (Figure 2; Supplementary Table S2).

An integrated predictive model for OS management

Data presented here and earlier (Causton *et al*, 2001) have clearly shown that OSR is a global phenomenon impacting a wide array of cellular processes encoded by at least 50% of all genes (Figure 2; Supplementary Figure S2 and S3; Supple-mentary Table S1). We have taken a step toward construction of a predictive model for global transcriptional coordination of the OSR. Briefly, using the cMonkey algorithm (Reiss *et al*, 2006), we integrated transcriptome changes, gene functional associations (phylogenetic profiles, chromosomal proximity, operon organization, metabolic networks, etc.), and *de novo* discovered conserved *cis*-regulatory motifs to identify subsets of genes that are conditionally co-regulated by OS (biclusters). Subsequently, we constructed an *e*nvironment and *g*ene *r*egulatory *in*fluence *net*work for OS (EGRIN$_{os}$) by performing linear regression and model selection using the Inferelator algorithm (Bonneau *et al*, 2006, 2007). Analysis of regulatory influences of TFs and the two OS agents on each bicluster within this model has recapitulated earlier known regulatory phenomena for managing OS and revealed new putative regulatory links among diverse cellular processes.

Discovery of co-regulated genes reveals new regulatory links among different OS components

Altogether, 1165 genes were grouped into 100 biclusters using the cMonkey algorithm (Supplementary Table S7). Using two examples, we show how this integrated the analysis of genes, environmental conditions, functional associations, and shared *cis*-regulatory motifs within individual biclusters has discovered numerous regulons and provided evidence for conditional co-regulation of diverse functions during OSR (Figure 3).

Example 1: Analysis of bicluster #84 (bc84) has provided evidence for the potential transcriptional co-regulation of *sod1* with several redoxins, a thioredoxin reductase, bacterioferri-tin, cysteine biosynthesis/repair enzymes, molecular chape-rones, and five genes with no matches to protein sequence or signature of characterized function. Though it has been shown that *sod1* and cysteine repair systems are part of the SoxRS regulon and Fe scavenging is part of the OxyR regulon (Imlay, 2008), global analysis has shown the two regulons to be overlapping (Farr and Kogoma, 1991; Zheng *et al*, 2001). Similarly, the gene composition of bc84 suggests that this regulon is analogous to a functional hybrid of the SoxRS and OxyR systems in *E. coli*. However, there are no orthologs for either of these regulators in *H. salinarum NRC-1* (Coulson *et al*, 2007). Subsequent regulatory network inference with Infer-elator has helped identify potential regulator(s) that mediate this control (see below). Notably, co-expression of the 23 genes was especially prominent in PQ-treated cells. Although this is consistent with the O_2^--specific function of some of these genes (e.g. *sod1*), it also suggests similar ROS-specific functions for some of the other genes.

Example 2: In bc12, we have discovered potential co-regulation of genes encoding siderophore biosynthesis, ferrichrome transport, a thioredoxin reductase, and eight earlier unknown function proteins. The regulatory link
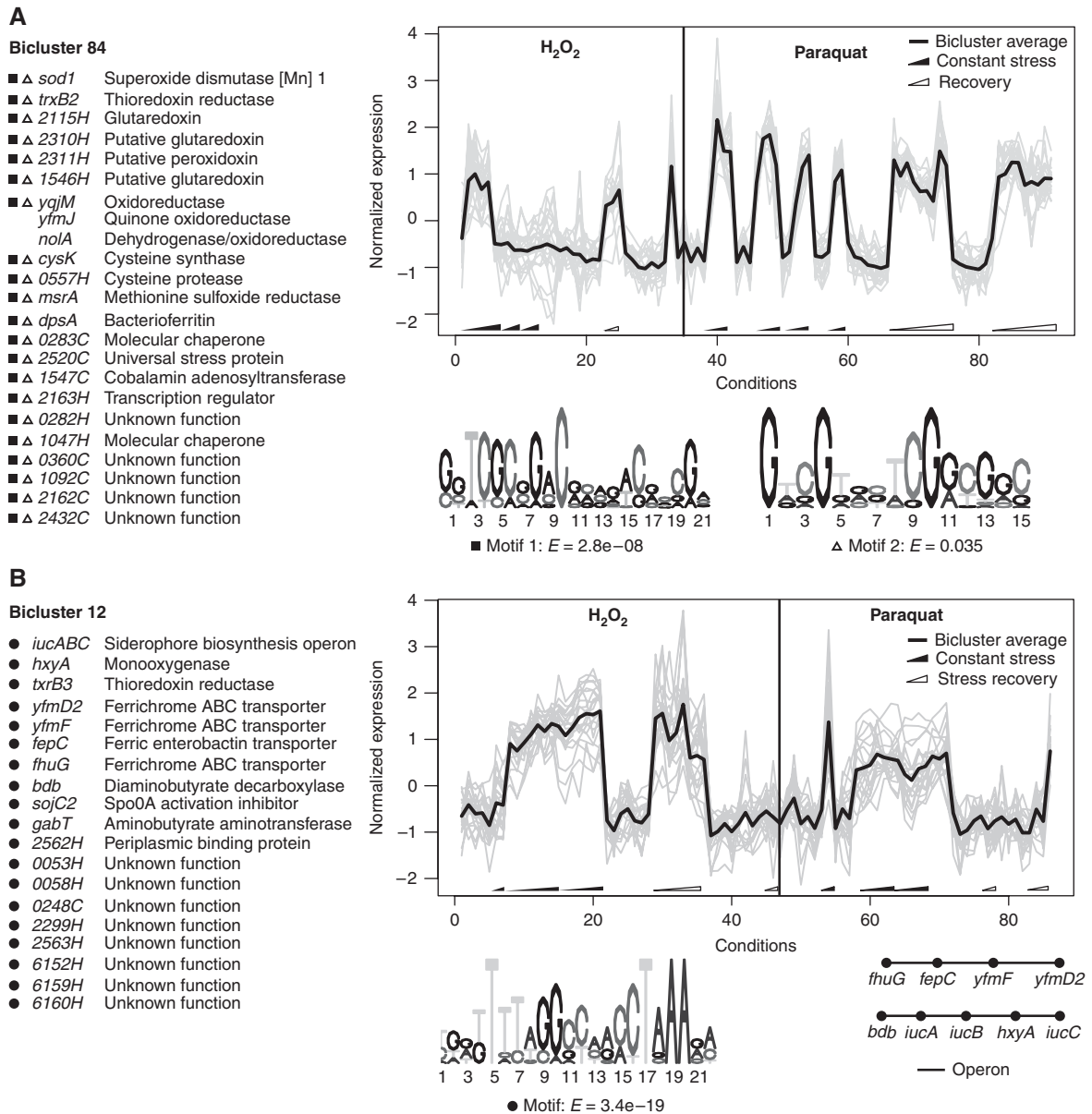
A

Bicluster 84

■ △ *sod1*   Superoxide dismutase [Mn] 1
■ △ *trxB2*   Thioredoxin reductase
■ △ *2115H*   Glutaredoxin
■ △ *2310H*   Putative glutaredoxin
■ △ *2311H*   Putative peroxidoxin
■ △ *1546H*   Putative glutaredoxin
■ △ *yqjM*   Oxidoreductase
     yfmJ   Quinone oxidoreductase
     nolA   Dehydrogenase/oxidoreductase
■ △ *cysK*   Cysteine synthase
■ △ *0557H*   Cysteine protease
■ △ *msrA*   Methionine sulfoxide reductase
■ △ *dpsA*   Bacterioferritin
■ △ *0283C*   Molecular chaperone
■ △ *2520C*   Universal stress protein
■ △ *1547C*   Cobalamin adenosyltransferase
■ △ *2163H*   Transcription regulator
■ △ *0282H*   Unknown function
■ △ *1047H*   Molecular chaperone
■ △ *0360C*   Unknown function
■ △ *1092C*   Unknown function
■ △ *2162C*   Unknown function
■ △ *2432C*   Unknown function

■ Motif 1: *E* = 2.8e−08   △ Motif 2: *E* = 0.035

B

Bicluster 12

● *iucABC*   Siderophore biosynthesis operon
● *hxyA*   Monooxygenase
● *txrB3*   Thioredoxin reductase
● *yfmD2*   Ferrichrome ABC transporter
● *yfmF*   Ferrichrome ABC transporter
● *fepC*   Ferric enterobactin transporter
● *fhuG*   Ferrichrome ABC transporter
● *bdb*   Diaminobutyrate decarboxylase
● *sojC2*   Spo0A activation inhibitor
● *gabT*   Aminobutyrate aminotransferase
● *2562H*   Periplasmic binding protein
● *0053H*   Unknown function
● *0058H*   Unknown function
● *0248C*   Unknown function
● *2299H*   Unknown function
● *2563H*   Unknown function
● *6152H*   Unknown function
● *6159H*   Unknown function
● *6160H*   Unknown function

● Motif: *E* = 3.4e−19

Figure 3 Discovery of conditionally co-regulated genes reveals novel physiological links. Conditionally co-regulated genes were discovered using the cMonkey algorithm (see text for details). (**A, B**) Shows two example biclusters: bc84 (23 genes) and bc12 (21 genes), respectively. The plots show mean and variance-normalized transcriptional changes (log$_{10}$ ratios) for all genes (gray) in each bicluster with an overlaid averaged profile (black). Filled triangles on *x* axis indicate time course analysis of responses during continued exposure to 25 mM H$_2$O$_2$ or 4 mM PQ. The open triangles, on the other hand, indicate time course analysis of recovery from 2 h exposure to 25 mM H$_2$O$_2$ or 4 mM PQ. Genes and their putative functions are indicated in the table. Sequence logos for the conserved motifs are shown in lower right of each panel, with numbers indicating nucleotide position and size of letters indicating relative conservation of bases. Genes possessing conserved DNA sequence motifs are marked with squares, triangles, or circles. (B) Lower right: operon-like organizations of nine genes within bicluster 12.

between siderophore biosynthesis and ferrichrome transport is not surprising given their shared functions in managing intracellular Fe pool (Andrews *et al*, 2003), and their conditional co-regulation during an OSR, especially H$_2$O$_2$ stress, in *E. coli* and *Bacillus subtilis* (Imlay, 2008). However, evidence for co-regulation of this process with a chromosome partitioning gene [*VNG6153G* (*sojC2*)], thioredoxin reductase [*VNG2301G* (*trxB3*)], and eight genes of unassigned functions is new information. A single conserved palindromic motif within the promoters of all genes within this bicluster

suggested that this regulon is under the direct control of a single TF (Figure 3).

In comparing the distribution of genes in the two biclusters discussed above, we also note that this integrated analysis has helped hypothesize condition-specific functions for genes of related function [redox homeostasis (e.g. thioredoxin reductase, glutaredoxin, and peroxiredoxins), 12 Fe-management genes, proteolysis, cobalamin biosynthesis, and O$_2^-$ metabolism] as well as putative functions for at least three genes (*VNG1092C*, *VNG0248C*, *VNG2299H*) of earlier unknown

function. Interactive exploration of all biclusters to enable similar discoveries is possible online at http://baliga.systemsbiology.net/drupal/content/egrin-oxidative-stress.

A unified model for global transcriptional coordination of responses to treatments with H_2O_2 and PQ

OSR regulators are typically associated with redox-active cofactors such as haem, flavins, pyridine nucleotides, Fe–S clusters, and redox-sensitive amino-acid side chains such as cysteinyl thiols (Green and Paget, 2004). Altogether, 26 TFs and 17 signal transducers [containing methyl-accepting chemotaxis protein (MCP)-signaling domain] in *H. salinarum NRC-1* have matches to motif signatures for these OS-sensing features (Zheng and Storz, 2000; Fomenko and Gladyshev, 2002; Paget and Buttner, 2003; Fontecave, 2006). A significant fraction of these regulators (21 TFs and 13 signal transducers) was differentially regulated in response to H_2O_2 and/or PQ treatments (Supplementary Table S5). Although the high degree of cross-regulation that we observed might result from chemical inter-conversions among ROS (Liochev and Fridovich, 2007), it is more likely because of regulators that sense a globally affecting parameter such as the overall redox status (Demple, 1997; Zheng and Storz, 2000) or metal ion composition of the cell (Touati, 2000; Moore and Helmann, 2005; Lee and Helmann, 2006). However, even though the trigger (e.g. redox status) for many of these regulators is the same, their mechanism of activation and the genes they regulate are nonetheless different. In *E. coli*, for instance, in response to O_2^- stress, SoxR gets activated through oxidation of its Fe–S cluster and regulates a specific subset of genes that is distinct from those controlled by OxyR, which is activated through oxidation of cysteine residue(s) under H_2O_2 stress (Zheng and Storz, 2000; Imlay, 2008). In our study as well, we have observed unique transcriptional responses, such as upregulation of three thioredoxins [*VNG1012H*, *VNG1259G* (*trxB2*), *VNG2600G* (*trxA2*)] and a DNA repair gene *VNG2473G* (*radA1*) by PQ, but not by H_2O_2, suggesting involvement of several ROS-specific regulatory mechanisms in mediating the global OSR.

We have taken a step toward a systems level model (Figure 4) that collectively explains these OS-induced gene-expression changes as a function of shared and unique influences of TFs and two ROS. These regulatory influences in EGRIN$_{OS}$ recapitulate the global transcriptional changes observed during an OSR (Supplementary Figure S5). EGRIN$_{OS}$ also provides meaningful insight into the interrelationships among stress-management systems and general aspects of physiology under H_2O_2 and PQ stress (Figure 4). The architecture of the model reveals that the OSR network has significant overlap with response networks that manage other kinds of stress. For instance, a common set of TFs are predicted to coordinate genes in bc6, which contains the putative dye-decolorizing peroxidase (*VNG0798H*), with those in bc84 (contains *sod1*) and bc12 (contains Fe-management proteins) (bc84 and bc12 are discussed in detail above). Likewise, OSR genes within bc26 (a monooxygenase, several thioredoxin reductases, methionine sulfoxide reductase *msrA*, cysteine synthetase *cysK*, and a putative protease) are positively influenced by the same putative TF (Imd1) that also negatively influences

transcription of cobalamin synthesis and ATP synthase genes in bc91. Finally, three biclusters containing genes of diverse redox-reactive functions (bc17—carotenoid biosynthesis; bc33—siderophore biosynthesis; bc71—antioxidant synthesis) are co-regulated by TFs with redox-sensing and metal-binding domains. In the following sections, we show how EGRIN$_{OS}$ can be used as a framework to formulate experimentally testable hypotheses for characterizing general and specific components of the OSR.

The architecture of this statistically inferred network (Figure 4A) can be used to formulate hypotheses regarding combinatorial control of cellular processes during an environmental response, OSR in this case. These hypotheses can be tested by validating physical interactions of TFs with promoters of genes they are predicted to regulate, and by analyzing transcriptional and phenotypic consequences of genetically perturbing TFs in the network. Using a combination of such experimental validations, we have overcome the complexities presented by extensive buffering within such networks because of multiple redundancies for regulation and stress management. We have validated regulatory influences of six TFs [Trh4 and five general transcription factors (GTFs—TFBb, c, d, f, and g)] in the OSR network by showing their physical interactions with promoters of target genes, and consequence of deleting some of these TFs on expression of these genes (TFBd and c) and, more importantly, on survival rate (TFBc) under OS. Specifically, we have validated combinatorial control of genes within the same bicluster (bc88) by multiple TFs (Trh4, TFBb, TFBf, and TFBg; Figure 4B; Supplementary Table S9), differential regulation of genes in different biclusters (bc3, bc81, bc72, and bc33) by the same TF (TFBd) (Figure 4C), and diminished capacity to withstand OS on deleting a predicted TF (TFBc) within this network (Figure 4D). The consequence of deleting TFBc on increased susceptibility to OS can now be further investigated in the context of its function in coordinating specific processes as predicted by EGRIN$_{OS}$.

Phenotypic analysis of mutants reveals a multi-tiered program for OS management

In addition to validating architecture of EGRIN$_{OS}$, we have also conducted phenotypic analysis of strains with in-frame chromosomal deletions in genes identified to be important in OS management based on their putative functions, their transcriptional changes in response to OS, and the EGRIN$_{os}$ model. Specifically, we investigated the functions of two SODs, three putative peroxidase/catalase genes, carotenoids, rhodopsins, and gas vesicles in OS management (Figures 5 and 6).

Two SODs (SOD1 and SOD2) offer protection against PQ treatment but not against H_2O_2

According to the EGRINos model, the two SOD genes are not co-regulated even by PQ treatment, which predominantly generates O_2^- stress in which their function is expected to be most relevant, suggesting distinct functions for the two orthologs. The co-regulation of *VNG1190G* (*sod1*) with genes encoding methionine sulfoxide reductase [*VNG1180G*
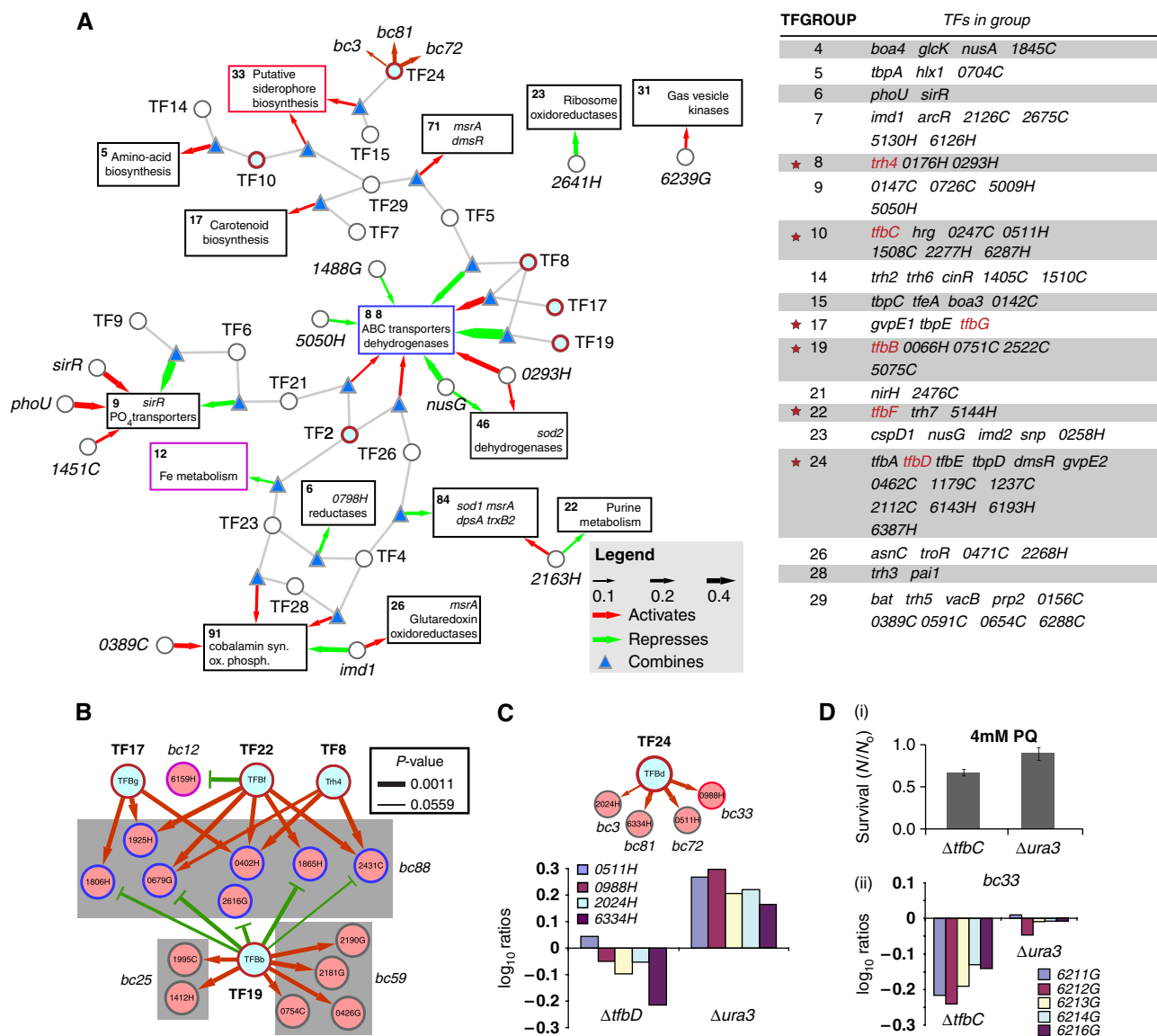
Figure 4 EGRIN_OS: environment and gene regulatory influence network for oxidative stress. (**A**) EGRIN_OS was constructed by applying the Inferelator algorithm to infer predictive regulatory influences of TFs and EFs (H_2O_2 and PQ) on biclusters of conditionally co-regulated genes discovered using cMonkey. To simplify visualization of this model, the network was filtered for biclusters with residuals < 0.4 and regulatory influence weights > 0.1 and restricted to physiological functions relevant to OS. Rectangles with numbers indicate specific biclusters; width of each box is proportional to number of conditions in that bicluster and height is proportional to number of genes. Likewise, width of each arrow is proportional to the strength of the regulatory influence, with red arrows indicating activation and green indicating repression. Circles indicate single TFs or groups of TFs. 'TF groups' are averaged expression profiles of their member TFs (see table). Triangles indicate a logical 'AND' combination of regulatory influences. A red star indicates that the influence of a TF (red font) within a particular group has been experimentally validated. Corresponding position of the TFgroups in the EGRINos network are indicated with a red border on relevant nodes. (**B**) Cross-correlation with independently measured protein–DNA interactions by ChIP-chip (Bonneau *et al*, 2007; Facciotti *et al*, 2007; Reiss *et al*, 2008) is consistent with the architecture of the network. TFs in different TFgroups bind promoters of genes within the same bicluster (bc88). Further, these TFs also bind promoters of genes in other biclusters that they are predicted to regulate. The network is drawn as a composite of P–D interactions and statistically inferred influences by Inferelator. Thickness of edges are proportional to significance of promoter binding in ChIP-chip experiments, whereas the activate (red arrows) and repress (green edges) influences are based on Inferelator predictions. (**C**) TFBd binds the promoters of at least four genes grouped into as many distinct biclusters. Consistent with its predicted influence a knockout in TFBd results in significantly lower transcript levels of these genes at all stages of growth in batch culture. This example validates the EGRIN_OS predicted regulation by TFBd and illustrates how a TF coordinates transcription of genes involved in different processes during OSR. (**D**) Finally, the deletion of TFBc, which is predicted to coordinate amino-acid metabolism and iron metabolism genes, results in increased sensitivity to 4 mM PQ [transcription factor-binding sites for the six TFs (indicated with red stars in panel A) are listed in Supplementary Table S9].

(*msrA*)], cysteine synthase [*VNG1301G* (*cysK*)], thioredoxin [*VNG1259G* (*trxB2*)], and a ferritin [*VNG2443G* (*dpsA*)] (see bc84) suggested a more significant function for this ortholog in providing protection against OS. In agreement with this

hypothesis, a knockout in *sod1*, but not *VNG1332G* (*sod2*), resulted in hypersensitivity to PQ treatment (Figure 5A and B). However, simultaneous deletions of both orthologs further increased sensitivity to O_2^- stress, relative to the $\Delta sod1$ mutant
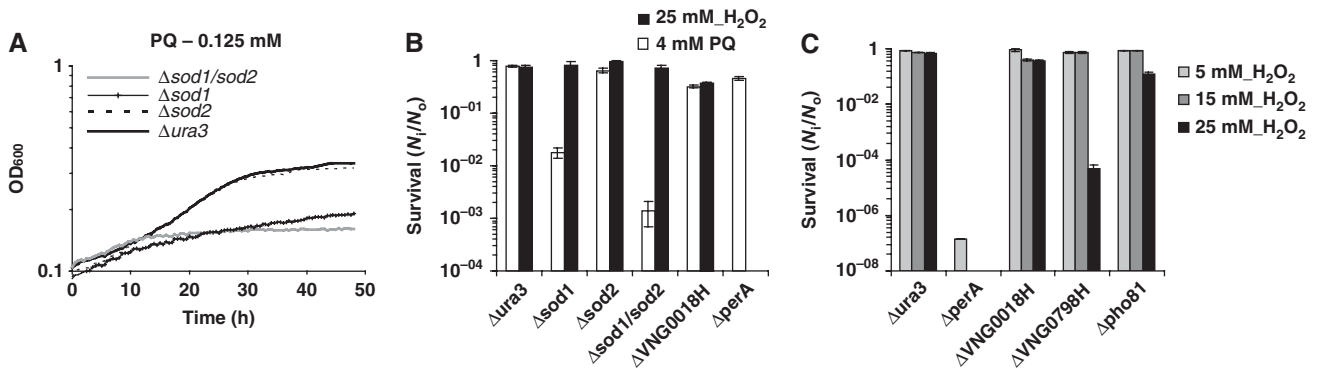
Figure 5 Phenotypic analyses of mutants under PQ and H_2O_2 stress. (**A**) Growth analysis of SOD single and double gene knockout mutants in the presence of 0.125 mM PQ. (**B**) Survival of mutants after a 2 h treatment with either 4 mM PQ or 25 mM H_2O_2. (**C**) Survival of mutants after 2 h treatment with 5, 15, or 25 mM H_2O_2. *H. salinarum* NRC-1 $\Delta ura3$ is the parent strain that was used as a control in all experiments.
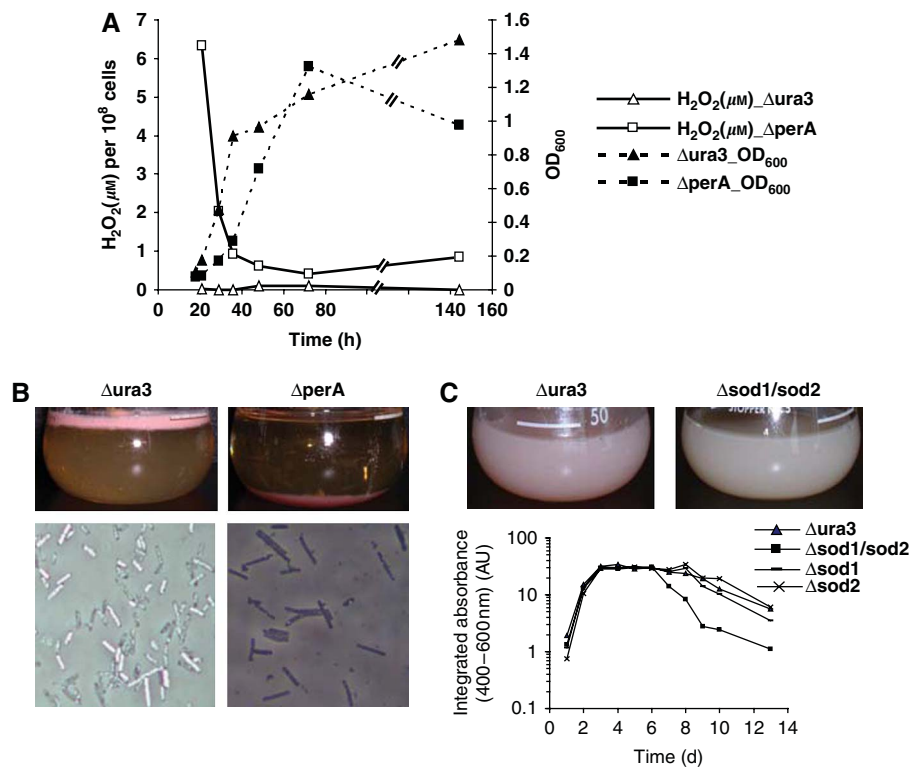

Figure 6 Secondary protective mechanisms against OS. (**A**) Endogenous H_2O_2 levels during aerobic growth of $\Delta ura3$ and $\Delta perA$ strains were quantified using the Amplex Red assay. Although H_2O_2 levels were consistently low throughout growth of the parent strain, as expected the levels were significantly higher in the peroxidase mutant. However, the unexpected growth of this mutant coincided with drop in H_2O_2 level, suggesting the presence of an alternate mechanism(s) to detoxify H_2O_2. (**B**) Defective gas vesicle biogenesis in the peroxidase mutant. To assay for flotation properties, cells were grown to stationary phase at 37°C and then left undisturbed (i.e. without shaking) at room temperature on the bench top. Although the parent $\Delta ura3$ strain floated to the surface, the peroxidase/catalase mutant sank to the bottom of the flask. Microscopy analysis confirmed that gas vesicles (observed as bright refractile bodies in the parent strain) are completely missing in the peroxidase/catalase mutant. (**C**) The function of carotenoids and other pigments was predicted to be important based on the bleached appearance of stationary phase cultures of the double $\Delta sod1/sod2$ mutant. This was confirmed on measuring and calculating a fourfold increase in the rate of degradation of pigments relative to single sod mutants ($\Delta sod1$, $\Delta sod2$) and the parent $\Delta ura3$ strain. Pigments were assayed using UV-VIS spectroscopy.

(Figure 5B). Together with the observation that *sod2* was upregulated only by treatment with a sub-lethal dose of PQ (Figure 2; Supplementary Figure S3), this suggested that this ortholog provides marginal protection against excessive O_2^- stress. However, this does not rule out a more significant function for this enzyme under specialized conditions (Valderas and Hart, 2001). Notably, unlike in other organisms (Carlioz and Touati, 1986), neither of the two SODs, individually or together, provided any protection against H_2O_2 stress (Figure 5B).

perA (peroxidase), *VNG0798H* (a putative 'dye-decolorizing' peroxidase), and VNG0018H (a protein of earlier unknown function) offer protection against H_2O_2 stress and some cross-protection to O_2^-

Consistent with its anticipated function in scavenging H_2O_2, deletion of the putative peroxidase/catalase gene *perA* resulted in poor growth under oxic conditions and hypersensitivity to H_2O_2 (Figure 5C; Supplementary Figure S6). The onset of growth of the $\Delta perA$ strain after a prolonged lag phase coincided with a corresponding drop in intracellular H_2O_2 content from ~ 6 to $< 2\,\mu M$ (levels observed in typical wild-type cell cultures; all measurements of H_2O_2 were normalized to 10^8 cells) (Figure 6A) (Gonzalez-Flecha and Demple, 1997; Seaver and Imlay, 2001). This suggested the presence of additional mechanism(s) to handle peroxide stress. The EGRIN$_{OS}$ model suggested two candidate genes: VNG0798H and VNG0018H. VNG0798H, which has a weak borderline match to a protein family signature for dye-decolorizing peroxidases (PF04261, *e*-value ~ 0.02), was upregulated by both H_2O_2 and PQ, and co-expressed with carotenoid biosynthesis enzymes, gas vesicle biogenesis proteins, and a putative heat shock protein (bc85) [http://baliga.systemsbiology.net/drupal/content/egrin-oxidative-stress]. Moreover, VNG0798H shares Inferelator-discovered regulatory influences with *sod1* and Fe-management proteins [section 'A unified model for global transcriptional coordination of responses to treatments with H_2O_2 and PQ'; Figure 4]. Likewise, VNG0018H, whose predicted protein structure (in lieu of absence of a sequence-based match to characterized proteins) matches that of a catalase (PDB: 1cf9A2; Mate *et al*, 1999) (Bonneau *et al*, 2004) was upregulated under H_2O_2 stress. Knockouts in these candidate genes validated their functions in providing partial protection against H_2O_2 stress (Figure 5C). Although deletion of *perA* resulted in complete loss of viability at 25 mM H_2O_2, deletion of *VNG0798H* and *VNG0018H* resulted in 99.9 and 62% reduction in survival, respectively (Figure 5C; Supplementary Figure S6). Furthermore, knockouts in *perA* and *VNG0018H* also resulted in 54 and 67% loss in survival, respectively, when challenged with 4 mM PQ (Figure 5B; Supplementary Figure S6).

Secondary mechanisms for OS management

The co-regulation of genes encoding rhodopsins, carotenoids, and gas vesicles with several known mechanisms to detoxify and manage ROS (e.g. in bc85—http://baliga.systemsbiology.net/drupal/content/egrin-oxidative-stress) suggested important functions for these processes in OS management (Figure 4). Culture characteristics of the *perA* and SOD mutants (Figure 6B and C) in conjunction with phenotypic analysis and transcriptomics further supported secondary protective functions for these functions and provided clues into their regulatory links to the primary protective mechanisms.

(a) *Rhodopsins and carotenoids have distinct functions in peroxide and superoxide stress management*: Pigments such as carotenoids, which are intermediates in synthesis of the retinal chromophore found in rhodopsins (Kushwaha *et al*, 1974), are known to act as antioxidants (Di Mascio *et al*, 1991). Consistent with this known function, the transcription of several genes involved in carotenoid biosynthesis [*VNG1458G* (*crtB1*), *VNG1684G* (*crtI1*), *VNG1755G* (*crtI2*), *VNG1680G* (*crtB2*), *VNG1465G* (*brp*)] and one opsin *VNG1467G* (*bop*) were upregulated during and/or after exposure to H_2O_2 and PQ (Figure 2M and N). This is also consistent with earlier knowledge that transcriptional regulation of these genes is influenced by redox status of the cell (Betlach *et al*, 1989; Yang and DasSarma, 1990; Shand and Betlach, 1991; Baliga *et al*, 2001). Furthermore, visual inspection of stationary phase cultures revealed a distinctly bleached appearance of the SOD double mutant—an observation that was confirmed by the fourfold increase in the oxidative degradation rate of pigments during normal growth of this strain relative to the wild-type strain (Figure 6C). The specific mechanism by which carotenoids scavenge ROS is unknown, although it has been speculated that they act through interference with reactions of damaging oxidizing agents (Woodall *et al*, 1997; Davison *et al*, 2002). Regardless, an increased rate of pigment bleaching in the SOD double mutant, but not the $\Delta perA$ mutant suggests a specific protective function for carotenoids in defense against O_2^- stress. This also partly explains the normal growth characteristics of the single and double SOD mutants under standard laboratory culturing conditions (Supplementary Figure S6). In contrast, depletion of all four rhodopsins [bacterio-rhodopsin (bR), halorhodopsin (hR), sensory rhodopsins I and II (sRI and sRII)] as well as two transducers (HtrI and HtrII) in *Pho81*, a strain constructed earlier for characterizing phototaxis mechanisms (Yao *et al*, 1994), resulted in increased peroxide toxicity (Figure 5C), but no difference in sensitivity to O_2^- (data not shown). In *H. salinarum NRC-1*, these proteins are involved in light-activated ion-pumping (bR and hR) and relocation of cells toward or away from particular wavelengths of radiation by phototaxis [sRI and II, and signal transducers (HtrI and II)]. This is a new function for these integral membrane proteins. The specific mechanisms by which carotenoids and rhodopsins provide protection against H_2O_2 and PQ stress will require further investigation.

(b) *Regulation of gas vesicle biogenesis is linked to peroxide stress*: H_2O_2 and PQ treatment induced transcription of genes encoding structural components of gas vesicles. Further, EGRIN$_{OS}$ suggested that under OS (especially H_2O_2 stress; see bc85) at least three of these genes [*VNG6236G* (*gvpG2*), *VNG6237G* (*gvpF2*), *VNG6239G* (*gvpE2*)] are co-induced with the dyp-type peroxidase (*VNG0798H*), a thioredoxin [*VNG5076G* (*trxA1*)], and a putative heat shock protein [*VNG1801G* (*hsp1*)]. The induction of purple membrane biogenesis and DMSO fermentation during OS, especially H_2O_2 treatment (Figure 2) suggests an OS-induced shift in physiology to one that is better suited for low oxygen conditions, so as to minimize the production of additional radicals. Induction of gas vesicle biogenesis under low O_2 tension is well known and speculated to be a mechanism used by *H. salinarum NRC-1* for scavenging traces of O_2 through floatation (Yang and DasSarma, 1990; Schmid *et al*, 2007). However, in the context of OS, flotation because of vesicle

production would be problematic, as it would increase exposure to O_2. Intriguingly, deletion of *perA* abolished gas vesicle biogenesis resulting in a sinking phenotype (Figure 6B)—a phenomenon also displayed by cyanobacteria that are subjected to OS (Berman-Frank *et al*, 2004). In *H. salinarum NRC-1*, this appears to be mediated through post-transcriptional suppression of gas vesicle biogenesis despite increased transcript levels of these genes under conditions of increased H_2O_2 stress.

Generalized and unique components of OSR

It is generally accepted that a significant proportion of cellular responses to diverse types of environmental stress (metals, radiation, starvation, etc.) is shared and constitutes a generalized OS component. We investigated this idea quantitatively by evaluating the degree to which the EGRIN model constructed from responses to perturbations in diverse EFs (six metals, O_2, light, UV and γ-radiation) was able to predict transcriptional changes induced by H_2O_2 and PQ treatment. First, using the measured values of just 72 TFs, 9 EFs, and their regulatory influences in the EGRIN model, we predicted transcriptional changes in 80% of all genes in 5000 resampled datasets of 140 experiments each. These datasets were randomly assembled from a pool of 722 new experiments that were not used to construct the model and that did not include any OS experiments (Supplementary Figure S7). This analysis showed the remarkable robustness with which the EGRIN model consistently made accurate global predictions with a mean error (RMSD) of 0.36 ± 0.01. Next, we used the model to make predictions of global gene-expression changes in the 140 experiments (including controls) that specifically investigated transcriptional responses to treatments with H_2O_2 and PQ. Remarkably, the model predicted global gene-expression changes induced by OS with similar accuracy, suggesting that most regulatory phenomena triggered by OS are also active during responses to other EFs. Historically, such responses that are triggered by diverse environmental stresses are lumped into a loosely defined 'general stress response.' Although it might be true that a significant fraction of this general stress response is an indirect consequence of the highly interconnected nature of biological networks, many genes are most certainly triggered by a particular injury or dysfunction. Notwithstanding this observation, a closer investigation revealed OS-specific coordinate regulation of important genes within several regulons that were not observed in responses to any other EFs. Specifically, regulons within 22 of the 67 biclusters within $EGRIN_{OS}$ (residuals <0.45) are partially or completely disrupted ($R^2 < 0.35$) in other environmental stress conditions such as treatments with sub-inhibitory doses of redox-active metals including Cu and Fe (Kaur *et al*, 2006), a sub-lethal dose of γ-radiation (Whitehead *et al*, 2006), or extreme changes in oxygen tension (Schmid *et al*, 2007) (Figure 7; Supplementary Table S10). The 288 genes within these 22 biclusters encode functions of detoxification, repair, Fe metabolism, nucleotide metabolism, and oligo/dipeptide ABC transporters. Although this analysis validates the notion that a significant fraction of cellular responses to diverse EFs does indeed constitute a generalized

component, it also reveals specific regulatory mechanism(s) for the management of excessive OS. The regulon within bc84 is a case in point. Genes within this regulon encode frontline defense mechanisms that are coordinately upregulated by PQ treatment, and to a lesser degree by H_2O_2 treatment, but not by redox-active metals, γ-radiation, or extreme changes in oxygen tension. Co-regulation of Fe-trafficking genes within bc12 is another example of this OS-specific regulatory phenomenon (Figure 7). It will be important to understand natural circumstances that produce such extreme OS, so we can better characterize the functional relevance of such OS-specific regulatory circuits for survival in a hypersaline environment. Especially important will be the dissection of the hierarchy of regulatory networks that coordinate the generalized and specific components of OSR as a function of the degree of OS. The $EGRIN_{OS}$ model lends itself to such an analysis by providing conditional interrelationships among TF activities in the form of joint influences on both response components of the OSR.
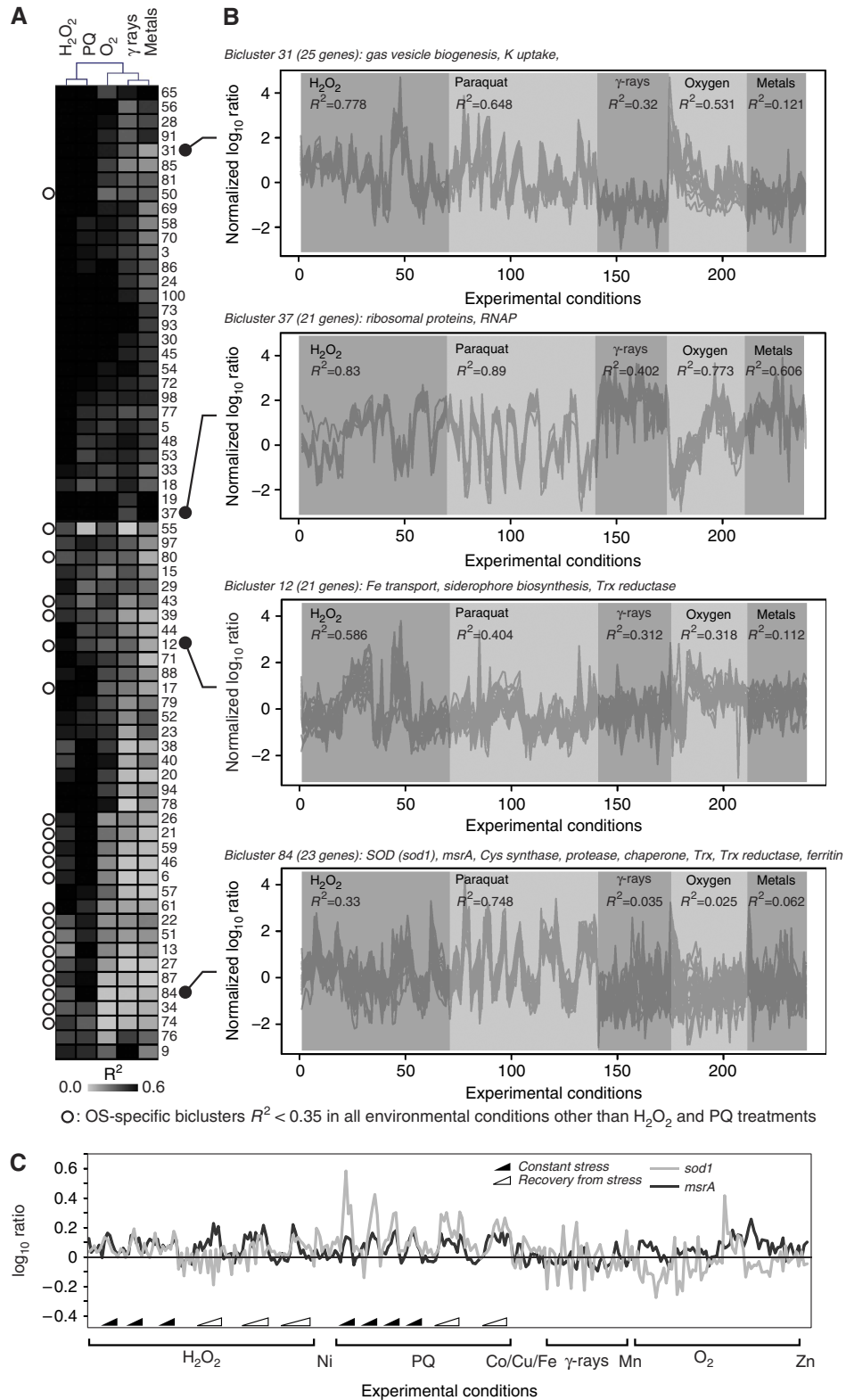
Summary and conclusion

Given the ubiquitous nature of OS, it is not entirely surprising that most organisms have evolved multiple lines of defense—both passive and active. Although many of these mechanisms have been extensively characterized in other organisms, our integrated systems approach has uncovered additional protective mechanisms in *H. salinarum* (e.g. VNG0798H and VNG0018H). Further, the systems approach has also revealed a structure and hierarchy to the OSR through conditional regulatory associations among various components of the response (Figures 4 and 5). Using this integrated approach, we can begin to synthesize an understanding of the multi-tiered program for management of H_2O_2 and O_2^- stress in *H. salinarum NRC-1*.

Briefly, H_2O_2 generated by normal metabolism is primarily handled by the peroxidase/catalase PerA; when H_2O_2 production exceeds detoxification capabilities of PerA, additional protection is provided by VNG0018H, rhodopsins, and VNG0798H, respectively (Figure 5). Uncontrolled accumulation of H_2O_2 such as on disruption of PerA causes cells to switch to anaerobic physiology, shutdown gas vesicle biogenesis, and sink away from oxygen (Figure 6). Coordinated upregulation of iron trafficking and management systems under severe H_2O_2 stress (bc12) might also serve to minimize Fenton reaction while keeping with the cellular demand for iron. O_2^- stress, on the other hand, is primarily managed by SOD1 with additional marginal protection from SOD2. When challenged with a sub-lethal dose of O_2^-, *H. salinarum NRC-1* increase the production of carotenoids to take advantage of their secondary function in scavenging ROS. Severe O_2^- stress results in the co-regulation of several frontline defense and repair functions including *sod1*, *msrA*, and *dpsA* (bc84) (Figure 3).

In addition to such O_2^--specific responses, there was also evidence of crosstalk in responses to H_2O_2 and O_2^- in the coordination of biclusters containing SOD1 (bc84) and VNG0798H (bc6) by the same set of regulatory influences (Figure 4). Likewise, two of the three peroxidases, *VNG0018H* and *perA*, also provide significant cross-protection against O_2^-

stress (Figure 5). Although this is to be expected as ROS are readily inter-converted such as by dismutation of O_2^- to H_2O_2, these network connections have also provided insights into the operational relationships in the crosstalk among two distinct

OS protection mechanisms. These operational relationships are further extended by the model to other aspects of physiology. For instance, the model reveals that the simultaneous upregulation of genes within bc6 (*VNG0798H*) and bc84

Figure A. Heatmap with columns H_2O_2, PQ, O_2, γ rays, Metals.

Bincluster 31 (25 genes): gas vesicle biogenesis, K uptake,
H_2O_2 $R^2=0.778$ | Paraquat $R^2=0.648$ | γ-rays $R^2=0.32$ | Oxygen $R^2=0.531$ | Metals $R^2=0.121$

Bicluster 37 (21 genes): ribosomal proteins, RNAP
H_2O_2 $R^2=0.83$ | Paraquat $R^2=0.89$ | γ-rays $R^2=0.402$ | Oxygen $R^2=0.773$ | Metals $R^2=0.606$

Bicluster 12 (21 genes): Fe transport, siderophore biosynthesis, Trx reductase
H_2O_2 $R^2=0.586$ | Paraquat $R^2=0.404$ | γ-rays $R^2=0.312$ | Oxygen $R^2=0.318$ | Metals $R^2=0.112$

Bicluster 84 (23 genes): SOD (sod1), msrA, Cys synthase, protease, chaperone, Trx, Trx reductase, ferritin
H_2O_2 $R^2=0.33$ | Paraquat $R^2=0.748$ | γ-rays $R^2=0.035$ | Oxygen $R^2=0.025$ | Metals $R^2=0.062$

R^2 0.0 — 0.6

O: OS-specific biclusters $R^2 < 0.35$ in all environmental conditions other than H_2O_2 and PQ treatments

C — Constant stress / Recovery from stress; sod1, msrA
Experimental conditions: H_2O_2, Ni, PQ, Co/Cu/Fe, γ-rays, Mn, O_2, Zn

(*sod1, msrA, dpsA*) under certain OS conditions is coordinated with downregulation of cobalamin synthesis and oxidative phosphorylation (bc91) in a biologically meaningful manner (Figure 4). We have validated some aspects of the architecture of this OSR network by confirming physical protein–DNA interactions of six TFs with promoters of genes they were predicted to influence by EGRIN$_{OS}$ (Figure 4B). Furthermore, we have also shown that deleting the TFs results in decreased transcript levels of predicted target genes and that disruption of this control can lead to decreased survival rate under OS (Figure 4C and D). It is notable that the five GTFs whose functions we have validated cannot directly sense ROS. This illustrates the importance of the EGRIN$_{OS}$ architecture and the functions GTFs have therein to globally coordinate various processes during OSR. This systems level insight would not be possible without integration of diverse global datasets. Finally, by comparing across active regulatory programs under diverse environmental stresses, we have quantitatively determined processes that are specifically triggered by extreme OS (Figure 7).

Materials and methods

Organism and growth conditions

H. salinarum NRC-1 (wild type), *H. salinarum NRC-1 Δura3* (parent for knockout strains), and all gene knockout strains were grown in complex medium (CM: 250 g/l NaCl, 20 g/l MgSO$_4$, 2 g/l KCl, 3 g/l sodium citrate, 10 g/l Oxoid brand bacteriological peptone) at 37°C and 220 r.p.m. shaking in Innova9400 incubator (New Brunswick). CM was supplemented with 50 mg/l uracil for strains constructed from a Δura3 background. Gene deletion mutants were constructed using a two-step in-frame gene replacement strategy as described earlier (Kaur *et al*, 2006) and rhodopsin-deficient strain, *Pho81*, has been characterized earlier (Yao *et al*, 1994).

Growth and survival assay

All strains were grown in CM with continuous shaking (200 r.p.m.) at 37°C until late log phase (OD ~0.8) and then further diluted into fresh medium to an optical density of 0.05. These cultures were then transferred to Honeycomb plate wells of Bioscreen C (Growth Curves USA, Piscataway, NJ). Different amounts of PQ (0, 0.125, 0.25, and 0.5 mM—final concentrations) or H$_2$O$_2$ (0, 4, 5, 6, and 7 mM—final concentrations) were added into individual wells. Samples were incubated at 37°C with continuous shaking and growth was monitored for 48 h in Bioscreen. For survival assay, *H. salinarum NRC-1* was exposed to either 0–100 mM H$_2$O$_2$ or 0–8 mM PQ, whereas knockout strains were exposed to only 25 mM H$_2$O$_2$ or 4 mM PQ for 2-h treatment. Cell viability was determined by counting colonies on agar plates. Sensitivity of Δura3, ΔperA, ΔVNG0798H, and *Pho81* were also tested with different concentrations of H$_2$O$_2$ (5, 15, 25 mM). Three independent measurements were made for each mutant.

Exposure to H$_2$O$_2$ and PQ for RNA preparation and microarray analysis

Two time courses were run to determine the transcriptional responses to (1) constant stress and (2) recovery of *H. salinarum NRC-1* to H$_2$O$_2$ and PQ. Mid-log phase cultures grown in flasks were treated with sub-lethal concentrations of 25 mM H$_2$O$_2$ or 4 mM PQ and incubated at 37°C with shaking for up to 240 min. During constant stress, culture aliquots (~4 ml) were collected over a time course (−1, 5, 10, 20, 40, 80, and 160 min), centrifuged (16 000 g, 90 s), and flash frozen. For recovery, cells were first treated for 2 h with either 25 mM H$_2$O$_2$ or 4 mM PQ, recovered by centrifugation, washed, and re-suspended in CM. Cultures were returned to the incubator with shaking and samples were taken at 0, 10, 20, 30, 40, 50, 60, 120, and 240 min and processed as described earlier. Analysis of temporal transcriptional changes (−1, 0, 5, 10, 20, 40, 80, 160, and 320 m) to sub-inhibitory concentrations of PQ (0.25 mM) was performed using the BioFlo110 modular bench-top fermentor (New Brunswick Scientific). Total RNA was prepared using the Absolutely RNA kit (Stratagene) according to manufacturer's instructions. Microarray slide fabrication, labeling with Alexa547 and Alexa647 dyes (Molecular Probes and Kreatech BV), hybridization, and washing were performed as described earlier (Baliga *et al*, 2004). Raw intensity signals were processed and resultant data were median normalized and evaluated for statistical significance of differential expression with significance of microarray (SAM) and variability and error estimates (VERA) algorithms (Ideker *et al*, 2000). In constant datasets, mRNA log$_{10}$ ratios were normalized to first condition (control) and data was filtered based on fold change >0.05, λ=15 in at least one condition. In recovery sets, data was filtered (fold change >0.05, λ=15) and compared with temporal changes in control experiments. A total of ~1400 genes met these criteria. Genes were further classified into different functional groups according to Kyoto Encyclopedia of Genes and Genomes, PFAM (http://pfam.sanger. ac.uk/), and clusters of orthologous groups (http://www.ncbi.nih. gov/COG). Analysis of microarray results was performed using hierarchical clustering and Dynamic Regulatory Events Miner (Ernst *et al*, 2007), which uses a hidden Markov model to construct dynamic models for condition-specific gene regulation. The complete micro-array dataset is available at http://www.ncbi.nlm.nih.gov/geo/query/ acc.cgi?acc=GSE17515.

H$_2$O$_2$ production during aerobic growth

H$_2$O$_2$ production was measured with Amplex Red H$_2$O$_2$ assay (Molecular Probes—A22188). Late log phase cultures of Δura3, ΔperA strains were diluted 1:100 in fresh CM and grown for six days. H$_2$O$_2$ levels were measured along the growth curve at different time points (21, 29, 36, 48, 72, and 144 h). The rate of H$_2$O$_2$ was normalized to the number of cells. The relation between OD$_{600}$ and cell number was calculated by counting cells in a flow cytometer.

Pigment analysis

Strains (Δura3, Δsod1, Δsod2, Δsod1/sod2) were grown in CM media at 37°C until late stationary phase. Aliquots (1 ml) were withdrawn from cultures at different time points (~24 h intervals), centrifuged at 16 000 g for 2 min. Pigments were extracted from cell pellets with 90% cold acetone and analyzed with UV-VIS spectrophotometer (Beckman

Figure 7 Coordination of frontline defense mechanisms under extreme OS. (**A**) Degree of co-regulation of genes within 67 biclusters (residuals <0.45) in diverse environmental stress conditions was evaluated by calculating correlations (R^2) among their transcript level changes in those experiments. The R^2-values were hierarchically clustered to identify the generalized and specific components of OSR. (**B**) Pearson's correlation (R) among mean and variance-normalized transcriptional changes for four representative biclusters are shown. Biclusters 31 and 37 are examples of the generalized stress response component of OSR with co-regulation across most environmental conditions. In contrast, co-regulation of genes within biclusters 12 and 84 is much more significant under severe OS conditions. For instance, genes of bc84 are co-regulated under severe OS resulting from treatment with sub-lethal dose PQ and to a lesser degree H$_2$O$_2$, but not on irradiation with a sub-lethal dose of γ-irradiation (Whitehead *et al*, 2006), subjecting cells to sudden and extreme changes in O$_2$ tension (Schmid *et al*, 2007) or treatment with sub-inhibitory dose of transition metals (Kaur *et al*, 2006). Genes within bc12, on the other hand, were better co-regulated on treatment with H$_2$O$_2$. Genes within both biclusters (especially bc84) encode important functions associated with frontline defense mechanisms that provide protection against OS (see Figure 3 and http://baliga.systemsbiology.net/drupal/content/ egrin-oxidative-stress for characteristics of biclusters). (**C**) A specific example of OS-specific co-regulation: two genes of bc84, *sod1* and *msrA*, are co-induced under severe OS—especially with PQ treatment—but not coordinately controlled by any other stressful environmental conditions.

Coulter—DU800). Absorption spectra were recorded and analyzed between 400 and 600 nm.

Gas vesicles visualization

Aliquots were harvested at various time points in $\Delta ura3$ and $\Delta perA$ strains and further diluted to an $OD_{600}=0.1$–0.2. Cells were then fixed by the addition of 0.25% formaldehyde (final concentration) and imaged with phase contrast microscopy.

Calculation of significance of enrichment

List of oxygen responsive genes was generated with principal component analysis of oxygen microarray experiment from earlier study (Schmid *et al*, 2007), which resulted in two categories of genes; one correlated (oxic genes—105) and other anti-correlated (anoxic genes—110) with oxygen. *P*-values were computed for enrichment of both oxic and anoxic genes among all OS responsive genes based on hyper-geometric distribution.

Motif search

Motifs conserved for various functions such as redox (CX_2S), Fe–S ($CX_2CX_2CX_3C$ and CX_3CX_2C), conserved cysteines residues of *oxyR* protein (CX_8C), and metal containing cysteine residues (CX_2C) along with PAS (PF00989, PF00785), GAF (PF01590), and MCP(PF00015)-signaling domain were identified from literature (Zheng and Storz, 2000; Fomenko and Gladyshev, 2002; Paget and Buttner, 2003; Fontecave, 2006). MatLab scripts were written to search the *H. salinarum NRC-1* proteome for matches to one or more of these conserved motifs (Supplementary Figure S4; Supplementary Table S5).

Accession sites

Access to modeling results online @: http://baliga.systems biology.net/drupal/content/egrin-oxidative-stress.
GEO accession number for microarray data: GSE17515 (http://www.ncbi.nlm.nih.gov/geo/query/acc.cgi?acc=GSE17515).

Supplementary information

Supplementary information is available at the *Molecular Systems Biology* website (http://www.nature.com/msb).

Conflict of interest

The authors declare that they have no conflict of interest.

References

Andrews SC, Robinson AK, Rodriguez-Quinones F (2003) Bacterial iron homeostasis. *FEMS Microbiol Rev* **27:** 215–237

Apel K, Hirt H (2004) Reactive oxygen species: metabolism, oxidative stress, and signal transduction. *Annu Rev Plant Biol* **55:** 373–399

Baliga NS, Bjork SJ, Bonneau R, Pan M, Iloanusi C, Kottemann MC, Hood L, DiRuggiero J (2004) Systems level insights into the stress response to UV radiation in the halophilic archaeon Halobacterium NRC-1. *Genome Res* **14:** 1025–1035

Baliga NS, Kennedy SP, Ng WV, Hood L, DasSarma S (2001) Genomic and genetic dissection of an archaeal regulon. *Proc Natl Acad Sci USA* **98:** 2521–2525

Berman-Frank I, Bidle KD, Haramaty L, Falkowski PG (2004) The demise of the marine cyanobacterium, Trichodesmium spp., via an autocatalyzed cell death pathway. *Limnol Oceanogr* **49:** 997–1005

Betlach MC, Shand RF, Leong DM (1989) Regulation of the bacterio-opsin gene of a halophilic archaebacterium. *Can J Microbiol* **35:** 134–140

Bonneau R, Baliga NS, Deutsch EW, Shannon P, Hood L (2004) Comprehensive *de novo* structure prediction in a systems-biology context for the archaea Halobacterium sp. NRC-1. *Genome Biol* **5:** R52

Bonneau R, Facciotti MT, Reiss DJ, Schmid AK, Pan M, Kaur A, Thorsson V, Shannon P, Johnson MH, Bare JC, Longabaugh W, Vuthoori M, Whitehead K, Madar A, Suzuki L, Mori T, Chang DE, Diruggiero J, Johnson CH, Hood L *et al* (2007) A predictive model for transcriptional control of physiology in a free living cell. *Cell* **131:** 1354–1365

Bonneau R, Reiss DJ, Shannon P, Facciotti M, Hood L, Baliga NS, Thorsson V (2006) The Inferelator: an algorithm for learning parsimonious regulatory networks from systems-biology data sets *de novo*. *Genome Biol* **7:** R36

Boyd JM, Drevland RM, Downs DM, Graham DE (2009) Archaeal ApbC/Nbp35 homologs function as iron-sulfur cluster carrier proteins. *J Bacteriol* **191:** 1490–1497

Brioukhanov AL, Netrusov AI, Eggen RI (2006) The catalase and superoxide dismutase genes are transcriptionally up-regulated upon oxidative stress in the strictly anaerobic archaeon Methanosarcina barkeri. *Microbiology* **152**(Part 6)**:** 1671–1677

Cabiscol E, Tamarit J, Ros J (2000) Oxidative stress in bacteria and protein damage by reactive oxygen species. *Int Microbiol* **3:** 3–8

Carlioz A, Touati D (1986) Isolation of superoxide dismutase mutants in Escherichia coli: is superoxide dismutase necessary for aerobic life? *EMBO J* **5:** 623–630

Causton HC, Ren B, Koh SS, Harbison CT, Kanin E, Jennings EG, Lee TI, True HL, Lander ES, Young RA (2001) Remodeling of yeast genome expression in response to environmental changes. *Mol Biol Cell* **12:** 323–337

Coulson RM, Touboul N, Ouzounis CA (2007) Lineage-specific partitions in archaeal transcription. *Archaea* **2:** 117–125

Davison PA, Hunter CN, Horton P (2002) Overexpression of beta-carotene hydroxylase enhances stress tolerance in Arabidopsis. *Nature* **418:** 203–206

Demple B (1997) Study of redox-regulated transcription factors in prokaryotes. *Methods* **11:** 267–278

Di Mascio P, Murphy ME, Sies H (1991) Antioxidant defense systems: the role of carotenoids, tocopherols, and thiols. *Am J Clin Nutr* **53** (1 Suppl)**:** 194S–200S

Ernst J, Vainas O, Harbison CT, Simon I, Bar-Joseph Z (2007) Reconstructing dynamic regulatory maps. *Mol Syst Biol* **3:** 74

Facciotti MT, Reiss DJ, Pan M, Kaur A, Vuthoori M, Bonneau R, Shannon P, Srivastava A, Donohoe SM, Hood LE, Baliga NS (2007) General transcription factor specified global gene regulation in archaea. *Proc Natl Acad Sci USA* **104:** 4630–4635

Farr SB, Kogoma T (1991) Oxidative stress responses in Escherichia coli and Salmonella typhimurium. *Microbiol Rev* **55:** 561–585

Finkel T (2005) Radical medicine: treating ageing to cure disease. *Nat Rev Mol Cell Biol* **6:** 971–976

Fomenko DE, Gladyshev VN (2002) CxxS: fold-independent redox motif revealed by genome-wide searches for thiol/disulfide oxidoreductase function. *Protein Sci* **11:** 2285–2296

Fontecave M (2006) Iron-sulfur clusters: ever-expanding roles. *Nat Chem Biol* **2:** 171–174

Gonzalez-Flecha B, Demple B (1997) Homeostatic regulation of intracellular hydrogen peroxide concentration in aerobically growing Escherichia coli. *J Bacteriol* **179:** 382–388

Grant CM (2001) Role of the glutathione/glutaredoxin and thioredoxin systems in yeast growth and response to stress conditions. *Mol Microbiol* **39:** 533–541

Green J, Paget MS (2004) Bacterial redox sensors. *Nat Rev Microbiol* **2:** 954–966

Hassan HM, Fridovich I (1979) Paraquat and Escherichia coli. Mechanism of production of extracellular superoxide radical. *J Biol Chem* **254:** 10846–10852

Ideker T, Thorsson V, Siegel AF, Hood LE (2000) Testing for differentially-expressed genes by maximum-likelihood analysis of microarray data. *J Comput Biol* **7:** 805–817

Imlay JA (2003) Pathways of oxidative damage. *Annu Rev Microbiol* **57:** 395–418

Imlay JA (2006) Iron-sulfur clusters and the problem with oxygen. *Mol Microbiol* **59:** 1073–1082

Imlay JA (2008) Cellular defenses against superoxide and hydrogen peroxide. *Annu Rev Biochem* **77:** 755–776

Joshi P, Dennis PP (1993) Characterization of paralogous and orthologous members of the superoxide dismutase gene family from genera of the halophilic archaebacteria. *J Bacteriol* **175:** 1561–1571

Kaur A, Pan M, Meislin M, Facciotti MT, El-Geweley R, Baliga NS (2006) A systems view of haloarchaeal strategies to withstand stress from transition metals. *Genome Res* **16:** 841–854

Kawakami R, Sakuraba H, Kamohara S, Goda S, Kawarabayasi Y, Ohshima T (2004) Oxidative stress response in an anaerobic hyperthermophilic archaeon: presence of a functional peroxiredoxin in Pyrococcus horikoshii. *J Biochem* **136:** 541–547

Kushwaha SC, Gochnauer MB, Kushner DJ, Kates M (1974) Pigments and isoprenoid compounds in extremely and moderately halophilic bacteria. *Can J Microbiol* **20:** 241–245

Lee JW, Helmann JD (2006) The PerR transcription factor senses H_2O_2 by metal-catalysed histidine oxidation. *Nature* **440:** 363–367

Limauro D, Pedone E, Galdi I, Bartolucci S (2008) Peroxiredoxins as cellular guardians in Sulfolobus solfataricus: characterization of Bcp1, Bcp3 and Bcp4. *FEBS J* **275:** 2067–2077

Limauro D, Pedone E, Pirone L, Bartolucci S (2006) Identification and characterization of 1-Cys peroxiredoxin from Sulfolobus solfataricus and its involvement in the response to oxidative stress. *FEBS J* **273:** 721–731

Liochev SI, Fridovich I (2007) The effects of superoxide dismutase on H_2O_2 formation. *Free Radic Biol Med* **42:** 1465–1469

Loiseau L, Ollagnier-de-Choudens S, Nachin L, Fontecave M, Barras F (2003) Biogenesis of Fe-S cluster by the bacterial Suf system: SufS and SufE form a new type of cysteine desulfurase. *J Biol Chem* **278:** 38352–38359

Mate MJ, Sevinc MS, Hu B, Bujons J, Bravo J, Switala J, Ens W, Loewen PC, Fita I (1999) Mutants that alter the covalent structure of catalase hydroperoxidase II from Escherichia coli. *J Biol Chem* **274:** 27717–27725

Metayer S, Seiliez I, Collin A, Duchene S, Mercier Y, Geraert PA, Tesseraud S (2008) Mechanisms through which sulfur amino acids control protein metabolism and oxidative status. *J Nutr Biochem* **19:** 207–215

Moore CM, Helmann JD (2005) Metal ion homeostasis in Bacillus subtilis. *Curr Opin Microbiol* **8:** 188–195

Oliver AE, Leprince O, Wolkers WF, Hincha DK, Heyer AG, Crowe JH (2001) Non-disaccharide-based mechanisms of protection during drying. *Cryobiology* **43:** 151–167

Outten FW (2007) Iron-sulfur clusters as oxygen-responsive molecular switches. *Nat Chem Biol* **3:** 206–207

Paget MS, Buttner MJ (2003) Thiol-based regulatory switches. *Annu Rev Genet* **37:** 91–121

Pahlman AK, Granath K, Ansell R, Hohmann S, Adler L (2001) The yeast glycerol 3-phosphatases Gpp1p and Gpp2p are required for glycerol biosynthesis and differentially involved in the cellular responses to osmotic, anaerobic, and oxidative stress. *J Biol Chem* **276:** 3555–3563

Perrone GG, Tan SX, Dawes IW (2008) Reactive oxygen species and yeast apoptosis. *Biochim Biophys Acta* **1783:** 1354–1368

Reindel S, Schmidt CL, Anemuller S, Matzanke BF (2006) Expression and regulation pattern of ferritin-like DpsA in the archaeon Halobacterium salinarum. *Biometals* **19:** 19–29

Reiss DJ, Baliga NS, Bonneau R (2006) Integrated biclustering of heterogeneous genome-wide datasets for the inference of global regulatory networks. *BMC Bioinformatics* **7:** 280

Reiss DJ, Facciotti MT, Baliga NS (2008) Model-based deconvolution of genome-wide DNA binding. *Bioinformatics* **24:** 396–403

Scheibner M, Hulsdau B, Zelena K, Nimtz M, de Boer L, Berger RG, Zorn H (2008) Novel peroxidases of Marasmius scorodonius degrade beta-carotene. *Appl Microbiol Biotechnol* **77:** 1241–1250

Schmid AK, Reiss DJ, Kaur A, Pan M, King N, Van PT, Hohmann L, Martin DB, Baliga NS (2007) The anatomy of microbial cell state transitions in response to oxygen. *Genome Res* **17:** 1399–1413

Seaver LC, Imlay JA (2001) Alkyl hydroperoxide reductase is the primary scavenger of endogenous hydrogen peroxide in Escherichia coli. *J Bacteriol* **183:** 7173–7181

Shand RF, Betlach MC (1991) Expression of the bop gene cluster of Halobacterium halobium is induced by low oxygen tension and by light. *J Bacteriol* **173:** 4692–4699

Shukla HD (2006) Proteomic analysis of acidic chaperones, and stress proteins in extreme halophile Halobacterium NRC-1: a comparative proteomic approach to study heat shock response. *Proteome Sci* **4:** 6

Stadtman ER (2006) Protein oxidation and aging. *Free Radic Res* **40:** 1250–1258

Stadtman ER, Moskovitz J, Levine RL (2003) Oxidation of methionine residues of proteins: biological consequences. *Antioxid Redox Signal* **5:** 577–582

Storz G, Imlay JA (1999) Oxidative stress. *Curr Opin Microbiol* **2:** 188–194

Sugano Y, Muramatsu R, Ichiyanagi A, Sato T, Shoda M (2007) DyP, a unique dye-decolorizing peroxidase, represents a novel heme peroxidase family: ASP171 replaces the distal histidine of classical peroxidases. *J Biol Chem* **282:** 36652–36658

Takahashi Y, Tokumoto U (2002) A third bacterial system for the assembly of iron-sulfur clusters with homologs in archaea and plastids. *J Biol Chem* **277:** 28380–28383

Temple MD, Perrone GG, Dawes IW (2005) Complex cellular responses to reactive oxygen species. *Trends Cell Biol* **15:** 319–326

Thorpe GW, Fong CS, Alic N, Higgins VJ, Dawes IW (2004) Cells have distinct mechanisms to maintain protection against different reactive oxygen species: oxidative-stress-response genes. *Proc Natl Acad Sci USA* **101:** 6564–6569

Toledano MB, Kumar C, Le Moan N, Spector D, Tacnet F (2007) The system biology of thiol redox system in Escherichia coli and yeast: differential functions in oxidative stress, iron metabolism and DNA synthesis. *FEBS Lett* **581:** 3598–3607

Touati D (2000) Iron and oxidative stress in bacteria. *Arch Biochem Biophys* **373:** 1–6

Tusher VG, Tibshirani R, Chu G (2001) Significance analysis of microarrays applied to the ionizing radiation response. *Proc Natl Acad Sci USA* **98:** 5116–5121

Valderas MW, Hart ME (2001) Identification and characterization of a second superoxide dismutase gene (sodM) from Staphylococcus aureus. *J Bacteriol* **183:** 3399–3407

Varghese S, Wu A, Park S, Imlay KR, Imlay JA (2007) Submicromolar hydrogen peroxide disrupts the ability of Fur protein to control free-iron levels in Escherichia coli. *Mol Microbiol* **64:** 822–830

Whitehead K, Kish A, Pan M, Kaur A, Reiss DJ, King N, Hohmann L, DiRuggiero J, Baliga NS (2006) An integrated systems approach for understanding cellular responses to gamma radiation. *Mol Syst Biol* **2:** 47

Woodall AA, Lee SW, Weesie RJ, Jackson MJ, Britton G (1997) Oxidation of carotenoids by free radicals: relationship

between structure and reactivity. *Biochim Biophys Acta* **1336:** 33–42

Yang CF, DasSarma S (1990) Transcriptional induction of purple membrane and gas vesicle synthesis in the archaebacterium Halobacterium halobium is blocked by a DNA gyrase inhibitor. *J Bacteriol* **172:** 4118–4121

Yao VJ, Spudich EN, Spudich JL (1994) Identification of distinct domains for signaling and receptor interaction of the sensory rhodopsin I transducer, HtrI. *J Bacteriol* **176:** 6931–6935

Zheng M, Storz G (2000) Redox sensing by prokaryotic transcription factors. *Biochem Pharmacol* **59:** 1–6

Zheng M, Wang X, Templeton LJ, Smulski DR, LaRossa RA, Storz G (2001) DNA microarray-mediated transcriptional profiling of the Escherichia coli response to hydrogen peroxide. *J Bacteriol* **183:** 4562–4570